

# A Uniform Viscoelastic-Plastic Constitutive Model for MD-PMMA at a Wide Temperature Range

Wei Liu\* and Wei-Hao Zhai

School of Mechanics, Civil Engineering & Architecture, Northwestern Polytechnical University, Xi'an 710129, China

**Abstract:** The deformation characteristics of MD-PMMA vary greatly at different temperatures. In the paper, whether a uniform model could be used to describe these complex characteristics was discussed. Tensile properties of MD-PMMA at the temperatures of -50°C, -25°C, 20°C, 60°C, 90°C were experimentally investigated. The entire deformation processes of PMMA were divided into four stages: elastic stage, viscoelastic stage, yielding stage and post-yielding stage. Strain softening and strain hardening phenomenon occurred in the yielding and post-yielding stage, it was the results of the competition between loading rate and plastic strain rate. A nonlinear model of activation dashpot was constructed, in the model, the evolution rate of plastic deformation was defined by Eyring's theory, and the actual stress was the difference between external applied stress and internal resistance stress caused by plastic strain. The above activation dashpot serially connected with the standard linear model (SLM) to identify elastic and viscoelastic characteristics. A two iterations integral algorithm was proposed to simplify the inter-coupling between the internal stress and the plastic strain, and the unknown parameters in the model could be easily fitted by the experimental data. This uniform viscoelastic-plastic model was demonstrated that could predict different deformation behaviors at a wide temperature range.

**Keywords:** Constitutive model, plastic strain, temperature, MD PMMA, internal stress.

## 1. INTRODUCTION

Multi-axes directional polymethyl methacrylate (MD-PMMA) is widely used to produce the transparencies (such as wind-shield or hatch) of aircraft, due to its good strength performance and anti-aging ability. It has been known that the PMMA's mechanical characteristic is sensitive to temperature and loading rate [1, 2]. On the conditions of different altitude and climates, the ambient temperature of aircraft could range from -55°C to 100°C [2]. In addition, during some complicated flight states, the transparent structures have to suffer continuous wind-stream loading or differential atmospheric pressure. For polymers, the phenomena of yielding and plastic flow are more likely to occur at warm temperature, but at low temperature, the material become hard and brittle. Therefore, whether a uniform model could be established to describe these complex characteristics should be further studied.

In the initial stage of the PMMA's deformation, viscoelasticity is always the research emphasis. Some types of viscoelastic elements (such as Maxwell element, Kelvin element or standard linear model (SLM)) are established to describe the polymers' nonlinear deformations before yielding [3, 4]. The concepts of stress relaxation modulus and creep compliance can be introduced from the above

viscoelastic elements, these concepts are often used to explain the influence of time scale and temperature scale on the deformation behaviors of polymer material, by the theory of time-temperature equivalence principle.

The strength and deformation of MD PMMA material are significantly correlative with strain rate. Transparencies structures of aircrafts are always weak regions for bird strikes, so the PMMA's dynamic properties at high strain rate also have been attracted many attentions [5-7]. The dynamic properties of PMMA can be tested by split Hopkinson bar. Some phenomena, such as strain strengthening, strain stiffening or high-speed brittleness, will occur at a high loading rate ( $10^1 \sim 10^3 \text{ s}^{-1}$ ). It has been test that the failure strain of PMMA is relatively small (usually less than 0.08) at high strain rate, and the plastic flow is not remarkable, some nonlinear viscoelastic models are applied to predict this fast deformation behavior.

At a lower strain rate ( $<10^1 \text{ s}^{-1}$ ), the stress-strain responses of PMMA exhibit many differences from viscoelastic-behaviors and dynamic-behaviors, such as a longer yielding process, post-yielding strain softening, strain hardening before fracture. Especially at a warm temperature (from the room temperature to the glass transition temperature), the polymer has a good ductility, so a large deformation will occur. Polymers are intrinsically strongly dependent on temperature, the initial Young's modulus and the yielding stress are found to decrease with increasing temperature [18], In order to characterize the mechanical behavior as a

\*Address correspondence to this author at the School of Mechanics, Civil Engineering & Architecture, Northwestern Polytechnical University, Xi'an 710129, China; Tel/Fax: +086-29-88431002; E-mail: liuweil@nwpu.edu.cn

function of temperatures and strain rate, many experimental studies have been carried out on different types of polymers [9, 10]. The investigations are mainly focused on three aspects: (1) the yielding criteria, (2) the formulation of coupled viscoelastic and plastic deformation, (3) the framework of stress-strain relations and related constitutive models.

By now, several theories have been proposed to explain plastic flow rule mechanisms for large deformation of polymers, such as Eyring model [10-12], molecular double-kink theory [13, 14] or free volume flow theory [15] *et al.* These theories were further expanded and developed by followed researchers to simulate some more detailed response when yielding and extreme large strain behaviors after yielding. A significant advance in modeling the strain softening of amorphous polymers was made by a variable called overstress or back-stress (an intermolecular resistance rate, pressure, temperature dependent) [13-16]. In the theory of overstress model, the proportion relation between the strain and corresponding stress response in equilibrium state was not valid, but there was a migration droved by some actual stresses; besides, the material parameters were not kept constant during the distortion process, but a function of strain and stress migration. Boyce *et al.* [16] proposed a finite elasto-viscoplastic material law on the rheology and the double-kink theory for the flow rule. Anand [17] used combined methods of macro- and micro-mechanics for PMMA material; they introduced internal-state variables that represent the local free-volume to capture the highly non-linear stress-strain behavior that precedes the yielding-peak and post-yielding strain softening more closely. Richeton *et al.* [19] proposed a cooperative model based on a strain rate/temperature superposition principle, the yielding behavior was identified as the energy of the secondary relaxation. Wu *et al.* [20] employed entropic network models borrowed from the statistical rubber elasticity theories. Arruda *et al.* [21] developed a temperature dependent strain hardening model which postulated that the network interactions forming part of polymer structure have a thermally equilibrated number. Dupaix *et al.* [22] investigated the rate-dependent stress-strain behavior of PETG at temperatures in and above the glass transition temperature. These works were further extended to the coupled thermo-mechanical set by Anand [23] and Miehe *et al.* [24], several micro-mechanically motivated internal variables were introduced to account for a more smooth transition after yielding. These coupled thermo-mechanical constitutive models were shown to perform well in reproducing the

features of strain softening and strain hardening effects. Some of these constitutive equations have been successfully executed into three-dimensional procedures.

However, the strain softening or strain hardening behaviors will not occur at cold temperatures, especially when the PMMA is exposed to the subzero temperatures, whether a uniform constitutive description is suitable for the description of the deformation behaviors at a more wide temperature range should be further investigated. In this paper, the tensile behaviors of MD PMMA at the temperatures of -50°C, -25°C, 20°C, 60°C, 90°C were tested. The Eyring's stress promote thermal activation theory was used to define the relation between plastic strain rate and temperatures, the evolution of plastic strain during the entire tensile process were discussed. A uniform constitutive model coupled with viscoelastic and plastic deformations were proposed, which can describe different deformation characteristics of polymers at a wide temperature range. The investigation will provide a more convenient way for the mechanical modeling of polymer material.

## 2. EXPERIMENT

A type of MD-PMMA material named "MDYB-3" was used in the test, MDYB-3 PMMA was often used to produce the hatch of aircraft, its glass transition temperature was 124°C. The MDYB-3 PMMA specimen was machined into the dog-bone shape (according to ASTM standard D638). The gauge length of the specimen was 30 mm. As PMMA is a type of soft and brittle material, a type of shoulder-lift fixture (Figure 1) was designed to clamp the specimen in the fatigue test to avoid unexpected fracture in the position of clamping.

Uniaxial tensile tests were carried out in the CSS 280 servo hydraulic universal machine. The investigation focused on deformation behaviors of MD PMMA at different temperature with low strain rate. Different temperature circumstances were realized by MT7006L Temperature Control Box (TCB), the operating temperature range of the TCB was -70°C~150°C, the maximal temperature fluctuation was  $\pm 0.2^\circ\text{C}$  when the TCB was kept at a constant temperature.

The TCB was installed in the sample-hold-region of CSS 280 (Figure 2). In order to cover the range of flight temperatures, the testing temperatures were selected



**Figure 1:** Shoulder-lift-clamps were applied to clamp the specimen.

as follows:  $-50^{\circ}\text{C}$ ,  $-25^{\circ}\text{C}$ ,  $20^{\circ}\text{C}$ ,  $60^{\circ}\text{C}$ ,  $90^{\circ}\text{C}$ . Before the tests, each specimen was kept in the specified temperature for half an hour at least. The extensometer and MTS-Test Star II system recorded the loading-displacement data for all specimens during the entire tensile test process. All specimens were polished carefully to ensure that the gauge section were parallel and smooth. Other details of the sample preparation, test steps and measures were carried out in accordance with ASTM standard D638.



**Figure 2:** Temperature Control Box (TCB) and CSS 280 servo hydraulic universal machine.

### 3. RESULTS

Monotonic tensile properties at the specified temperatures were measured; the tensile stress-strain

curves of PMMA at tested temperatures were shown in Figure 3. The MD PMMA undergone a dramatic change in stiffness and deformation, there was a great difference between its tension behaviors at different temperatures.

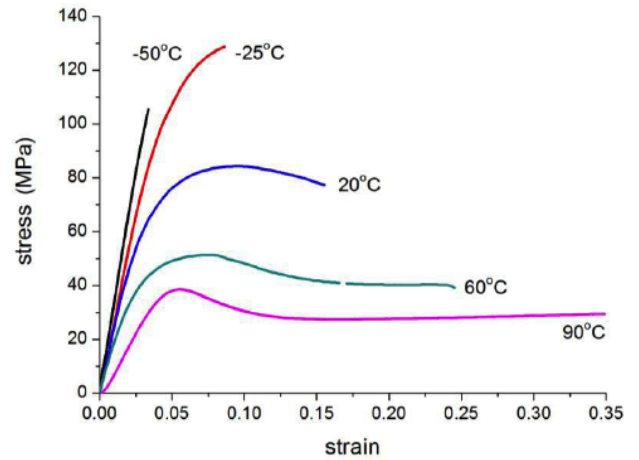


**Figure 3:** Tensile stress-strain curves of MDYB-3 PMMA at different temperatures.

The stress-strain curve was almost linear, and the failure strain was only 0.033 at  $-50^{\circ}\text{C}$ . Experiment showed that brittle fracture occurred at the temperatures of  $-50^{\circ}\text{C}$  and  $-25^{\circ}\text{C}$ , nearly no plastic transition was observed from the test specimens, fracture happened on the stress peak point. The MD PMMA exhibited a bigger modulus at a lower temperature, but the failure strain was smaller at a lower temperature, which resulted in an even higher failure stress of  $-25^{\circ}\text{C}$  than that of  $-50^{\circ}\text{C}$ .

When the temperature increased, the elastic modulus trended to decrease, the deformation showed an obvious nonlinear deformation characteristics before yielding, a yielding point appeared in the deformation curve of  $20^{\circ}\text{C}$ , the failure strain increased to 0.17. At higher temperature, its modulus dropped sharply, and a phenomenon of strain softening was observed after yielding, there was a maximal stress peak before softening (at  $60^{\circ}\text{C}$  and  $90^{\circ}\text{C}$ ), and necking phenomenon appeared in the test of  $90^{\circ}\text{C}$  and the failure strain extended to 0.347, which indicated that the MD PMMA became softer at higher temperature. Interestingly with the strain further increased, a faint strain hardening phase occurred in the final loading stage at the temperature of  $90^{\circ}\text{C}$  (seen in Figure 3), this phase was considered as an oriented-hardening for the polymer's inherent rheological property [18-20], but this final hardening phase was not reflected at lower temperatures (such as  $60^{\circ}\text{C}$ ) because of a relatively smaller strain deformation before fracture.

## 4. DISCUSSION

### 4.1. Eyring Model

The microscopic mechanism for plastic deformation of glassy high polymer can be explained by the Eyring transition state theory [10]. The theory is based on the hypothesis of thermal activating plastic deformation promoted by applied stress, which assumes that a quantity of macromolecule segments conformations in polymer are driven by the activation energy, and this thermally activation is motivated by adjacent molecular chain elements during loading process. The deformation is the process of the macromolecule segments moving from one equilibrium position to an adjacent one.

In general, when the material does not bear any stress, a dynamic balance will exist in the polymer, the frequencies and speeds of crossing over the potential barrier from the two directions (plus or minus direction) are equivalent (Figure 4). But when an applied stress  $\sigma$  is applied, the height of barrier in the applying force direction will change the first order variation can be valued at  $\pm v\sigma$  approximately [11, 12], here the parameter  $v$  is a proportional constant with volume dimension, which is called as activated volume. Therefore, the plastic deformation can be treated as an orientate transition movement (crossing over the potential barrier of Van-der-Waals bond) of a certain amount of activation volumes (here, the amount is assumed in span of  $V_a$ ) in polymer.

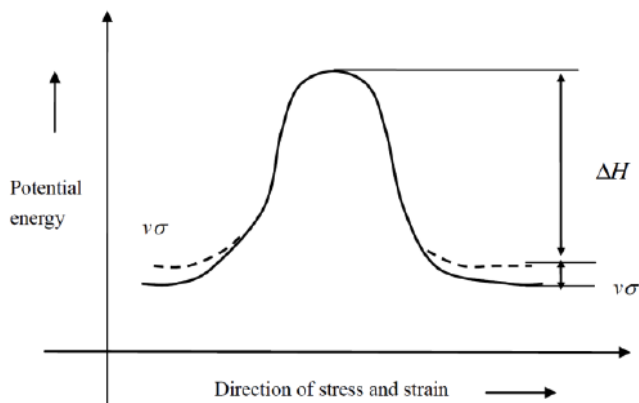


**Figure 4:** Schematic sketch of Eyring's stress motivate thermal activation model.

The plastic strain rate  $\dot{\epsilon}_p$  is defined as the direct proportional of net forward-flow-rate when external stress  $\sigma$  is applied; it can be expressed as follows [10]:

$$\dot{\epsilon}_p = \frac{4}{3} \left( \frac{V_a kT}{V_m h} \right) e^{-\frac{\Delta G}{kT}} \sinh \left( \frac{\xi V_a \sigma}{kT} \right) \quad (1)$$

Here,  $\sigma$  is the applied tension or compression stress,  $T$  is the absolute temperature of loading environment.  $\xi$  is the conversion factor for the slipping-shear-stress converting to the tension or compression stress, it can be valued as 0.427 for MD PMMA material [25],  $h$  and  $k$  is the Planck constant and Boltzmann constant respectively:

$$k = 1.38 \times 10^{-23} \text{ J/K}, \quad h = 6.63 \times 10^{-34} \text{ J}\cdot\text{s} = 4.14 \times 10^{-15} \text{ eV}\cdot\text{s},$$

$V_m$  is volume of molecular chain,  $\frac{V_a}{V_m}$  is the activated volume fraction involved in one transition,  $\Delta G = \Delta H - T\Delta S$  is the height of potential barrier, that is activated free energy,  $\Delta H$  is the activate energy and  $\Delta S$  is the activation entropy.

In order to find out the influence on the general characteristics of deformation, the specimen at a medium temperature is specially investigated. Figure 5 is the tensile stress-strain curve of MDYB-3 PMMA at 20°C. It can be seen that, from loading to final fracture, the entire deformation process at 20°C could be divided into four stages: elastic stage, viscoelastic stage, yielding stage and post-yielding stage. In the initial stage of the deformation, this specimen is dominated by elastic deformation, then the elastic deformation and viscoelastic deformation increases with the applied stress, and later, during the yielding stage, there is a maximal stress peak  $\sigma_s$  in loading response curve, which indicated that the plastic deformation play a leading role at the yielding point. After the yielding point (post-yielding process), the material turns into buckling deformation stage age ( $(d\sigma/d\epsilon) < 0$ ) [12, 25], which is shown by the phenomenon of strain softening. The elastic strain, viscoelastic strain and plastic strain dominates different actions in the above four stages during the entire loading process. The axial plastic deformation will

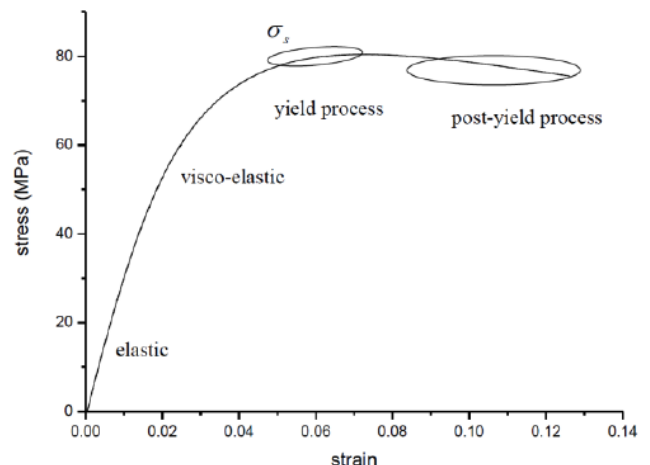


**Figure 5:** Monotonic tensile stress-strain of MDYB-3 PMMA at temperature of 20°C.

decrease when its rate  $\dot{\epsilon}_p$  is exceeded the external loading rate  $\dot{\epsilon}$ , which will result in a decrease of stress. So the yielding point of stress-strain curve is actually the mechanical state of  $\dot{\epsilon}_p = \dot{\epsilon}$  [12, 26].

From Figure 5, the yielding stress of MD PMMA is much larger than 1 MPa (that is  $\sigma_s \gg 1$  MPa), in order to simplify the function operation, the hyperbolic sine function can be calculated by exponential function [11],

$$\sinh\left(\frac{\xi V_a \sigma_s}{kT}\right) \approx \frac{1}{2} e^{\frac{\xi V_a \sigma_s}{kT}} \quad (2)$$

In order to simplify the expression, a symbol of  $A_f$  is introduced to denote the expressions before the exponential function in formula (1),

$$A_f = \frac{4}{3} \left( \frac{V_a kT}{V_m h} \right) e^{-\frac{\Delta G}{kT}} \quad (3)$$

$A_f$  is regarded as an intrinsic factor which integrate the frequency, activation energy and activation entropy of the orientate transition movement actually, its value span is  $10^{-8} \sim 10^{-12} \text{s}^{-1}$  generally, so substitute the equations (2), (3) into formula (1), the following can be obtained,

$$\dot{\epsilon}_p \approx \frac{A_f}{2} e^{\frac{\xi V_a \sigma_s}{kT}} \quad (4)$$

where  $V_a$  is activation volume, a material constant for activation viscous-pot. It is a characterization variable for describing the thermal activation plastic deformation transition volume participated in once cross-over potential energy movement.

The deformation process of MDYB-3 PMMA goes through four stages of elastic, viscoelastic, yielding and post-yielding (Figure 5). In the different stages, different types of strain rates are occupying the dominant position. For the situation of a constant imposed loading rate, elastic and viscoelastic strain rates decrease gradually when the material enters the yielding phase, but the plastic strain rate  $\dot{\epsilon}_p$  increases gradually until it occupies the total strain change completely at the yielding point. So the yielding point of polymer is not the starting point of plastic deformation, but the dominant point for plastic deformation. Based on this view, the yielding behavior of polymer material is actually a competition between the external loading rate  $\dot{\epsilon}$  and plastic strain rate  $\dot{\epsilon}_p$ . When the plastic rate  $\dot{\epsilon}_p$  reaches the imposed loading rate  $\dot{\epsilon}$ , the bearing capacity begins to declines, it is known as the strain-

softening phenomenon for polymer materials. By taking the logarithm of equation (4), the following equation can be obtained:

$$\ln(\dot{\epsilon}_p) \approx \ln(\dot{\epsilon}) \approx \ln\left(\frac{A_f}{2}\right) + \left(\frac{\xi V_a}{kT}\right) \sigma_s \quad (5)$$

The activation dashpot parameters of  $A_f$  and  $V_a$  can be obtained from equation (5) by fitting the experimental data of  $\lg(\dot{\epsilon}) - \sigma_s$  with various loading rates under imposed temperature condition [27].

#### 4.2. Plastic Deformation Characteristics

The plastic strains  $\epsilon_p$  can be obtained by using the integral algorithm from the Equation (4), and the comparisons between the plastic strain and the total strain are displayed in Figure 6. It can be seen that the plastic strain increases gradually after the total strain progresses to a certain point, the  $\epsilon_p$  starts to occur when the total strain is about up to 0.025 (the total strain of the demonstrated specimen (20°C) is 0.02381), then it grows until its amount reaches to 0.02~0.03 at the yielding point, it occupies the 30% proportion of total strains approximately at the yielding point.

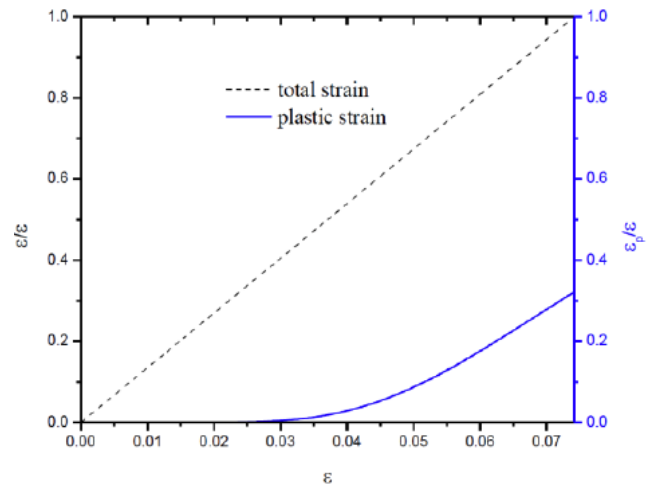
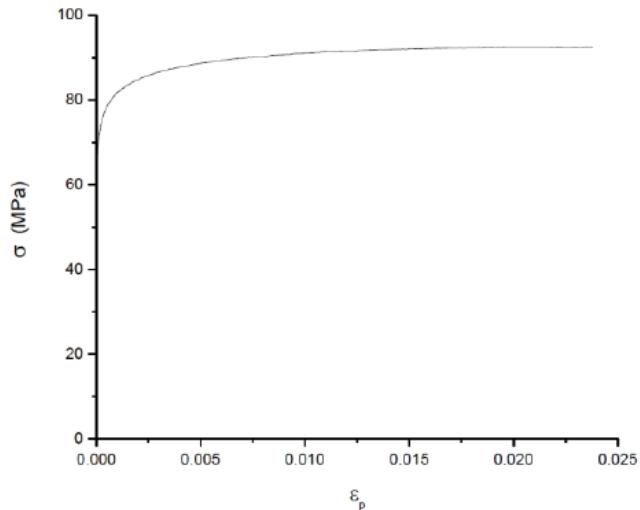


Figure 6: The ratio between the plastic strain and the total strain before yielding.

The curve of plastic strain  $\epsilon_p$  varying with the applied stress  $\sigma$  is shown in Figure 7, it can be seen that when the applied stress is greater than  $\frac{3}{4} \sigma_s$ , the  $\epsilon_p$  will be increased rapidly, which indicates that the yielding point of polymer materials is not starting point for the plastic deformation, but the state point of plastic deformation is beginning to play a dominant role.



**Figure 7:** The relation between plastic strain and applied stress.

The growth progress of plastic strains with the total strains rate is displayed in Figure 8. If the loading rate keeps as a constant, between the initial loading point and the yielding point, the plastic strain rate  $\dot{\epsilon}_p$  will begin to increase gradually when the total strain rises at the site of  $\epsilon \approx 0.02$ , and occupies the total deformation rate completely when reaches the yielding point.

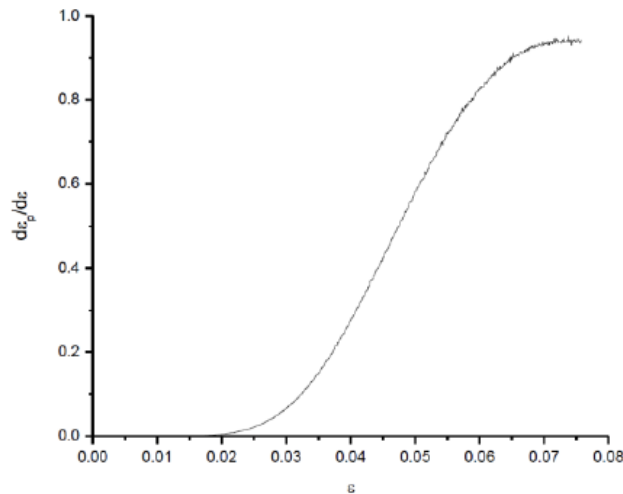


**Figure 8:** The proportion of plastic strain rate  $\dot{\epsilon}_p$  with loading rate  $\dot{\epsilon}$  before yielding.

The deformation before yielding point can be regarded mainly as the elastic and visco-elastic strains (Figure 6), but during the yielding process, the plastic strain growth adds a additional non-linear part (Figure 7), and the plastic strain rate becomes to be a dominant factor for the deformation during the yielding process gradually. So the yielding point is a state of the plastic strain rate mastering the current distortion process, rather than initial or start point of plastic strain

(Figure 8). In the yielding stage, the plastic strain  $\dot{\epsilon}_p$  continuously accelerates, until up to the critical point of  $\dot{\epsilon}_p = \dot{\epsilon}$ , the applied loading rate  $\dot{\epsilon}$  is occupied by the plastic strain  $\dot{\epsilon}_p$  completely, and then strain softening phenomenon occurs, which is regarded as an inherent characteristic for polymer materials.

### 4.3. Viscoelastic-Plastic Constitutive Model

Although the traditional viscoelastic model is hard to describe the yielding and softening behaviors, considering that all the deformation of MD PMMA undergoes elastic and viscoelastic phases firstly, so the standard linear model (SLM) is retained in the paper. The softening effect associated with plastic strain, more complicated mechanical elements should be serially or parallelly connected with the coupled viscoelastic element. Here, in order to simulate the viscoelastic-plastic phenomenon during the tension process, a model of an activation dashpot serially connecting with a SLM is constructed in Figure 9, the model assumes that the total strain  $\epsilon$  are combined by two parts: the viscoelastic strain  $\epsilon_v$  and plastic strain  $\epsilon_p$ . The parameters  $E, \tau_v$  in the SLM indicate the viscoelastic part, and the Eyring model (Eq. (4)) is used to represent the plastic part. These parameters in the model vary with the temperature  $T$  and loading rate  $\dot{\epsilon}$ , so actually Figure 9 is a temperature and rate related, viscoelastic and plastic coupled nonlinear constitutive model.

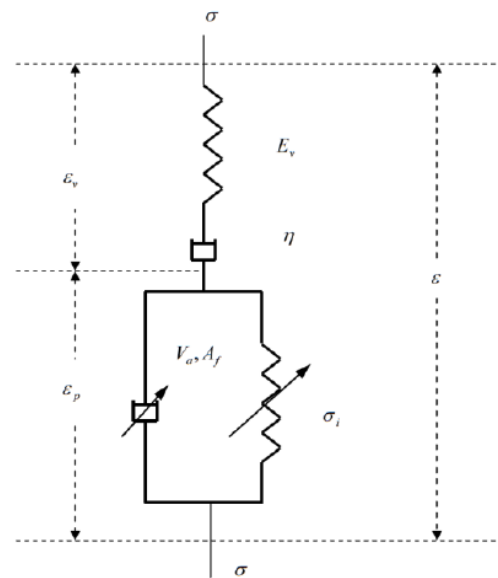


**Figure 9:** The viscoelastic-plastic coupled nonlinear constitutive model for MD PMMA.

The power function is usually used to express the internal stress (over stress) caused by the resistance of plastic strain [12, 16]:

$$\sigma_i = \zeta \varepsilon_p^n \quad (6)$$

where  $\zeta$  and  $n$  is the coefficient and exponent respectively. Taking the softening effect into account, the plastic strain rate can be represented as:

$$\dot{\varepsilon}_p = A_f \sinh\left(\frac{\xi V_a}{kT}(\sigma - \sigma_i)\right) \quad (7)$$

According to the constitutive equation of SLM and activation dashpot, the complete constitutive equations for the proposed model in Figure 9 can be written in differential form:

$$\sigma + \tau_v \dot{\sigma} = E_v \dot{\varepsilon}_v = E_v (\dot{\varepsilon} - \dot{\varepsilon}_p) \quad (8)$$

$$\dot{\varepsilon}_p = A_f \sinh\left(\frac{\xi V_a}{kT}(\sigma - \sigma_i)\right) \quad (9)$$

$$\sigma_i = \zeta \sigma_p^n \quad (10)$$

Integral transformation can be applied to the above equations:

$$\sigma = \int_0^t (\dot{\varepsilon} - \dot{\varepsilon}_p) \exp\left(-\frac{t-t'}{\tau_v}\right) dt' \quad (11)$$

$$\dot{\varepsilon}_p = A_f \sinh\left(\frac{\xi V_a}{kT}(\sigma - \zeta \varepsilon_p^n)\right) \quad (12)$$

where  $t$  is the total time for tension process,  $t'$  is the integration variable.

On the condition of constant loading rate ( $\dot{\varepsilon} = const$ ), the corresponding distortion  $\delta'_t$  can be derived as  $\delta'_t = \dot{\varepsilon} \cdot t'$ , so the original integration variable  $t'$  could be replaced by the variable  $\delta'_t$ , and the follow transition expressions can be obtained:

$$\sigma = E_v \int_0^{\delta_t} \left\{ 1 - \frac{A_f}{\dot{\varepsilon}} \sinh\left(\frac{\xi V_a (\sigma(\delta'_t) - \zeta \varepsilon_p^n(\delta'_t))}{kT}\right) \right\} \exp\left(-\frac{\delta_t - \delta'_t}{\delta_t \tau_v}\right) d\delta'_t \quad (13)$$

$$\varepsilon_p = \int_0^{\delta_t} \frac{A_f}{\dot{\varepsilon}} \sinh\left(\frac{\xi V_a (\sigma(\delta'_t) - \zeta \varepsilon_p^n(\delta'_t))}{kT}\right) d\delta'_t \quad (14)$$

where  $\delta_t$  is the total distortions of MD PMMA specimen in the tension test.

As for unloading process, if the strain rate  $\dot{\varepsilon}$  is assumed to be a negative constant, the above constitutive model can be used to describe the unloading behavior:

$$\sigma = E_e (\varepsilon - \varepsilon_p) - E_v \tau_v \dot{\varepsilon} \left[ 1 - \exp\left(-\frac{\varepsilon_v^R - \varepsilon_v}{\dot{\varepsilon} \tau_v}\right) \right] + E_v \int_0^{\varepsilon_p^R} \left\{ 1 - \frac{A_f}{\dot{\varepsilon}} \sinh\left(\frac{\xi V_a (\sigma(\delta'_t) - \zeta \varepsilon_p^n(\delta'_t))}{kT}\right) \right\} \exp\left(-\frac{(\varepsilon_v^R - \varepsilon_v) - \delta'_t}{\dot{\varepsilon} \tau_v}\right) d\delta'_t \quad (15)$$

where  $\varepsilon_v^R$  is the visco-elastic strain corresponding with the unload point.

#### 4.4. Model Parameters and Simulation

The values of  $V_a$  and  $A_f$  at different temperatures can be fitted by equation (5). In the equations of (13) and (14), the plastic strain  $\varepsilon_p$  and the actual stress  $\sigma$  were inter-coupling; the stress response of the equation (13) can be executed by three numerical iterations approximately. Firstly, initial value of internal stress is set as zero, that is  $\sigma_i = \zeta \varepsilon_p^n = 0$  (in the initial loading stage, the deformation is assumed totally elastic, and the plastic strain do not occur), zero internal stress is substituted into equation (14) and a zero<sup>th</sup> order approximation of  $\varepsilon_p$  (defined as  $\varepsilon_p^{(0)}$ ) could be obtained. Then the value of  $\varepsilon_p^{(0)}$  is substituted into equation (13) again and a zeroth order approximation of stress response  $\sigma$  (defined as  $\sigma_p^{(0)}$ ) could be obtained. Secondly, in order to obtain other unknown parameters in the above integral equations, the experimental stress-strain data should be fitted, and the tested  $\sigma - \varepsilon$  curve is transformed to  $\delta - \varepsilon$  curve (Figure 7) and  $\dot{\varepsilon}_p - \varepsilon$  curve (Figure 8). Thirdly, the relation between the total strain  $\delta$  and the approximate corresponding stress response  $\sigma^{(2)}$  can be obtained by two iterative Simpson integral computations by following algorithms:

$$\sigma^{(1)} = E_v \int_0^{\delta} \left\{ 1 - \frac{A_f}{\dot{\varepsilon}} \sinh\left(\frac{\xi V_a \sigma^{(0)}}{kT}\right) \right\} \exp\left(-\frac{\varepsilon - \delta}{\dot{\varepsilon} \tau_v}\right) d\delta \quad (16)$$

$$\varepsilon_p^{(1)} = \int_0^{\varepsilon} \frac{A_f}{\dot{\varepsilon}} \sinh\left(\frac{\xi V_a \sigma^{(1)}}{kT}\right) d\varepsilon \quad (17)$$

$$\varepsilon_p^{(2)} = \int_0^{\varepsilon} \frac{A_f}{\dot{\varepsilon}} \sinh\left(\frac{\xi V_a (\sigma^{(1)} - \zeta (\varepsilon_p^{(1)})^n)}{kT}\right) d\varepsilon \quad (18)$$

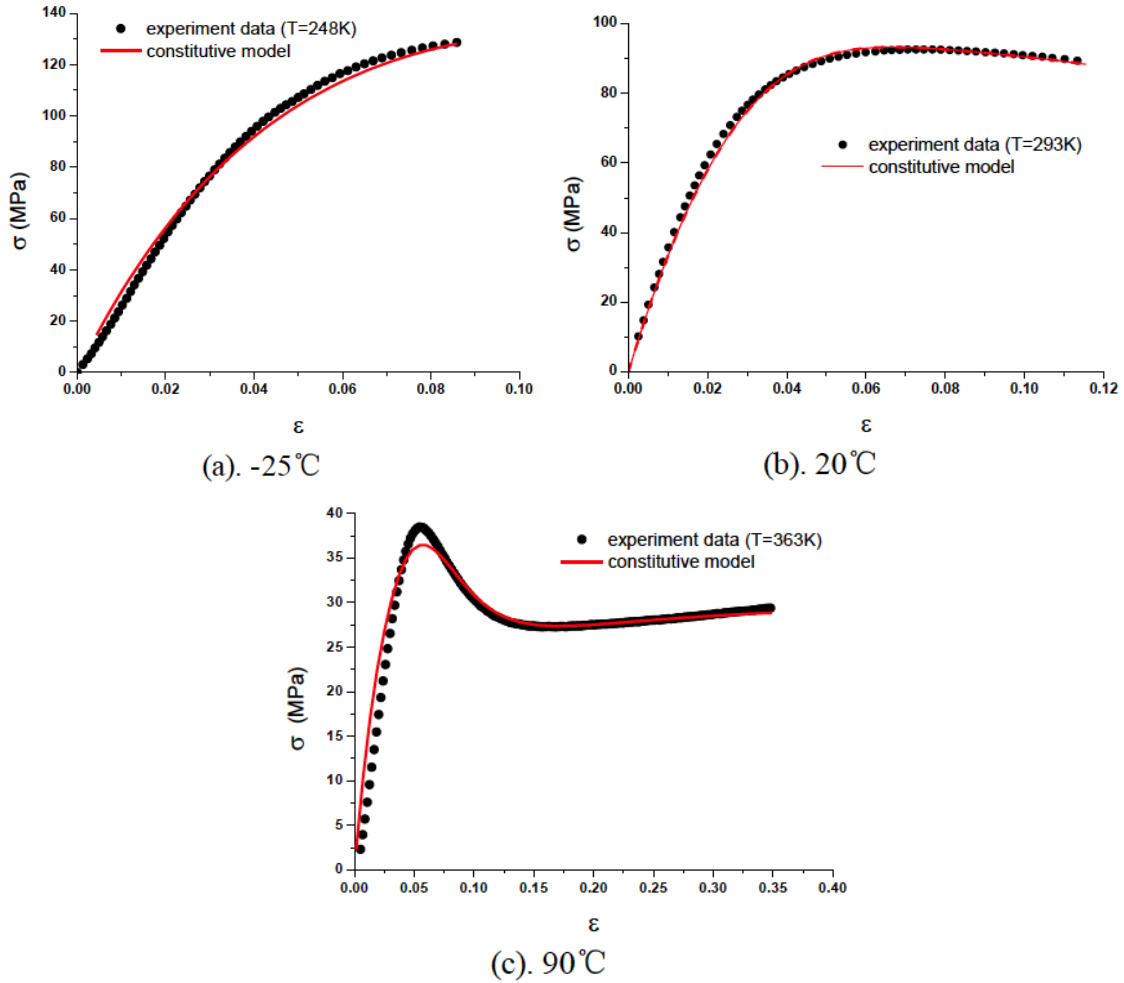


**Figure 10:** The compare of experiment data and the uniform constitutive model at different temperatures. (a) -25°C, (b) 20°C, (c) 90°C.

$$\sigma^{(2)} = E_v \int_0^\delta \left\{ 1 - \frac{A_f}{\dot{\epsilon}} \sinh \left( \frac{\xi V_a}{kT} \left( \sigma^{(1)} - \zeta (\epsilon_p^{(2)})^n \right) \right) \right\} \exp \left( -\frac{\epsilon - \delta}{\dot{\epsilon} \tau_v} \right) d\delta \quad (19)$$

Finally, the other unknown parameters in the above equations, such as  $\zeta$ ,  $n$ ,  $\tau$ ,  $E_e$ ,  $E_v$ , can be obtained by nonlinear data fitting of the actual tested data. In order to simplify the calculation, the following symbols are defined:

$$P_1 = \frac{A_f}{\dot{\epsilon}}, P_2 = \frac{\xi V_a}{kT}, P_3 = \zeta, P_4 = n, P_5 = \dot{\epsilon} \tau.$$

The fitted curve and the original experimental curve are basically in coincidence after about 200 cycles iterative computation, the error of least square fitting is constant on 1.92083 (20°C), it can be seen that the proposed constitutive model can represent the whole process from loading to fracture accurately, and the effect of loading rate is also included in the model.

The material parameters of MDYB-3 PMMA at other tested temperatures could be obtained by the same

implementations. The tension behaviors of PMMA predicted by the proposed model are plotted in Figure 10, it can be seen that the theoretical predictions from proposed uniform constitutive model agrees with the experimental data excellently.

### 5. CONCLUSION

Temperature influences MD-PMMA's deformations behavior remarkably. The stress-strain curve is almost linear at -50°C and -25°C, plastic transition is not observed and fracture happens on the stress peak point. But at warmer temperatures, the deformation undergoes four stages: elastic, viscoelastic, yielding and post-yielding. The phenomena of strain softening and strain hardening occur successively at 90°C.

The viscoelastic strain rate and plastic strain rate dominate different action during the entire loading process. The yielding point of polymer is not the starting point of plastic deformation, but the dominant

point for plastic deformation, and the yielding behavior of polymer material is actually a competition between the external loading rate and plastic strain rate, the actual stress was the difference between external applied stress and internal resistance stress caused by plastic strain.

A uniform constitutive model coupled with viscoelastic and plastic deformations has been established, the power form internal stress related with plastic strain can be applied to capture the nonlinear strain softening characteristics after yielding. The two iterations integral algorithm is effective for simplifying the inter-coupling between the internal stress and the plastic strain, and the material parameters in the model are easily fitted by the experimental data. An excellent agreement has demonstrated that the proposed uniform constitutive model can be used to predict different stress-strain behavior at a wide temperature range.

## ACKNOWLEDGEMENT

This project is supported by National Natural Science Foundation of China (Grant No. 51305350), the Natural Science Foundation of Shaanxi Province (No.2013JM6011) and the Basic Researches Foundation of NWPU (No.3102014JCQ01045).

## REFERENCES

- [1] Wu HY, Ma G, Xia YM. Experimental study of tensile properties of PMMA at intermediate strain rate. *Mater Lett* 2004; 58: 3681-5. <http://dx.doi.org/10.1016/j.matlet.2004.07.022>
- [2] Guo WG, Shi FF. Deformation and failure behavior of MDYB-3 oriented PMMA glass under different loading conditions. *Acta Aeronautica Et Astronautica Sinica* 2008; 29: 1517-25.
- [3] Zhang CT, Moore ID. Nonlinear mechanical response of high density polyethylene. Part II: Uniaxial constitutive modeling. *Poly Eng & Sci* 1997; 37: 414-20. <http://dx.doi.org/10.1002/pen.11684>
- [4] Zhang Y, Huang ZP. A model for the nonlinear viscoelastic behavior of amorphous polymers. *Mech Res Commun* 2004; 31: 195-202. <http://dx.doi.org/10.1016/j.mechrescom.2003.09.002>
- [5] Segreti M, Rusinek A, Klepaczko JR. Experimental study on puncture of PMMA at low and high velocities, effect on the failure mode. *Polym Test* 2004; 23: 703-18. <http://dx.doi.org/10.1016/j.polymertesting.2004.01.005>
- [6] Forquin P, Nasraoui M, Rusinek A, *et al.* Experimental study of the confined behaviour of PMMA under quasi-static and dynamic loadings. *Int J Impact Eng* 2012; 40: 46-57. <http://dx.doi.org/10.1016/j.ijimpeng.2011.09.007>
- [7] Xie ZQ, Zhang PP. On the Dynamic compressive mechanical properties and strain rate related constitutive model of PMMA material. *J Exp Mech* 2013; 28: 220-6.
- [8] Varghese AG, Batra RC. Constitutive equations for the thermomechanical deformations of glassy polymers. *Int J Solids Struct* 2009; 46: 4079-94. <http://dx.doi.org/10.1016/j.ijsolstr.2009.08.006>
- [9] Fleischhauer R, Dal H, Kaliske M, *et al.* A constitutive model for finite deformation of amorphous polymers. *Int J Mech Sci* 2012; 65: 48-63. <http://dx.doi.org/10.1016/j.jimecs.2012.09.003>
- [10] Chaboche JL. A review of some plasticity and viscoplasticity constitutive theories. *Int J Plasticity* 2008; 24: 1642-93.
- [11] Eyring H. Viscosity, plasticity, and diffusion as examples of absolute reaction rates. *J Chem Phys* 1936; 4: 283-91. <http://dx.doi.org/10.1063/1.1749836>
- [12] Zhu XX. Yielding and plastic deformation of solid polymers. *Adv Mech* 1992; 22: 449-63.
- [13] Ayoub G, Zairi F, Abdelaziz MN, *et al.* Modeling large deformation behavior under loading-unloading of semicrystalline polymers: Application to a high density polyethylene. *Int J Plasticity* 2010; 26: 329-47. <http://dx.doi.org/10.1016/j.ijplas.2009.07.005>
- [14] Argon AS. A theory for the low temperature plastic deformation of glassy polymers. *Philos Mag* 1973; 28: 839-65. <http://dx.doi.org/10.1080/14786437308220987>
- [15] Ozgen UC. Modeling deformation behavior of polymers with viscoplasticity theory based on overstress. *Int J Plasticity* 2005; 21: 145-60. <http://dx.doi.org/10.1016/j.ijplas.2004.04.004>
- [16] Boyce M, Parks D, Argon AS. Large inelastic deformation of glassy polymers. Part I: rate dependent constitutive model. *Mech Mater* 1988; 7: 15-33. [http://dx.doi.org/10.1016/0167-6636\(88\)90003-8](http://dx.doi.org/10.1016/0167-6636(88)90003-8)
- [17] Anand L, Gurtin ME. A theory of amorphous solids undergoing large deformations, with application to polymeric glasses. *Int J Solids Struct* 2003; 40: 1465-87. [http://dx.doi.org/10.1016/S0020-7683\(02\)00651-0](http://dx.doi.org/10.1016/S0020-7683(02)00651-0)
- [18] Haward RN, Thackray G. The use of a mathematical model to describe isothermal stress-strain curves in glassy thermoplastics. *Proc Royal Soc Lond Ser A Math Phys Sci* 1968; 302: 453-72.
- [19] Richeton J, Ahzi S, Vecchio KS, *et al.* Influence of temperature and strain rate on the mechanical behavior of three amorphous polymers: Characterization and modeling of the compressive yielding stress. *Int J Solids Struct* 2006; 43: 2318-35. <http://dx.doi.org/10.1016/j.ijsolstr.2005.06.040>
- [20] Wu PD, Giessen VD. On improved network models for rubber elasticity and their applications to orientation hardening in glassy polymers. *J Mech Phys Solids* 1993; 41: 427-56. [http://dx.doi.org/10.1016/0022-5096\(93\)90043-F](http://dx.doi.org/10.1016/0022-5096(93)90043-F)
- [21] Arruda EM, Boyce MC, Jayachandran R. Effects of strain rate, temperature and thermomechanical coupling on the finite strain deformation of glassy polymers. *Mech Mater* 1995; 19: 193-212. [http://dx.doi.org/10.1016/0167-6636\(94\)00034-E](http://dx.doi.org/10.1016/0167-6636(94)00034-E)
- [22] Dupaix RB, Boyce MC. Constitutive modeling of the finite strain behavior of amorphous polymers in and above the glass transition. *Mech Mater* 2007; 39: 39-52. <http://dx.doi.org/10.1016/j.mechmat.2006.02.006>
- [23] Anand L, Ames NM, Srivastava V, *et al.* A thermo-mechanically coupled theory for large deformations of amorphous polymers. Part I: Formulation. *Int J Plasticity* 2009; 25: 1474-94. <http://dx.doi.org/10.1016/j.ijplas.2008.11.004>
- [24] Miehe C, Diez JM, Goktepe S, *et al.* Coupled thermoviscoplasticity of glassy polymers in the logarithmic strain space based on the free volume theory. *Int J Solids Struct* 2011; 48: 1799-817. <http://dx.doi.org/10.1016/j.ijsolstr.2011.01.030>
- [25] Zhu XX, Zhu GR, Huang XS, *et al.* The nonlinear thermoviscoelastic plastic constitutive relations for an

- aeronautical PMMA. *Acta Aeronautica Et Astronautica Sinica* 1992; 13: 594-601.
- [26] Ward IM. *The mechanical properties of solid polymers*. Beijing: Science Press 1988.
- [27] Gao ZZ, Liu W, Liu ZQ, *et al.* Experiment and simulation study on the creep behavior of PMMA at different temperatures. *Polym Plast Technol* 2010; 49: 1478-82. <http://dx.doi.org/10.1080/03602559.2010.496429>

---

Received on 16-06-2015

Accepted on 22-09-2015

Published on 28-10-2015

DOI: <http://dx.doi.org/10.6000/1929-5995.2015.04.03.2>

© 2015 Liu and Zhai; Licensee Lifescience Global.

This is an open access article licensed under the terms of the Creative Commons Attribution Non-Commercial License (<http://creativecommons.org/licenses/by-nc/3.0/>) which permits unrestricted, non-commercial use, distribution and reproduction in any medium, provided the work is properly cited.